

A Perturbative Approach to Predict Eye Diagram Degradation in Differential Interconnects Subject to Asymmetry and Nonuniformity

Paolo Manfredi*, Xinglong Wu[†], Flavia Grassi[†], Dries Vande Ginste*, and Sergio A. Pignari[†]

*Electromagnetics Group, Department of Information Technology, IDLab, Ghent University – imec
Technologiepark-Zwijnaarde 15, 9052 Gent, Belgium
E-mail: paolo.manfredi@ugent.be

[†]EMC Group, Department of Electronics, Information and Bioengineering, Politecnico di Milano
Piazza Leonardo Da Vinci 32, 20133 Milano, Italy

Abstract—This paper proposes a novel framework for the signal integrity (SI) analysis of differential interconnects affected by nonuniformity and geometrical asymmetry. The pertinent nonuniform transmission-line (TL) equations are solved in the frequency domain by means of a perturbation technique, which allows interpreting the resulting response degradation as a perturbation with respect to the response of a reference uniform differential line (DL) with averaged per-unit-length (p.u.l.) parameters. Following this interpretation, the problem is recast as a standard TL equation for the reference uniform line with additional equivalent distributed sources that account for the perturbative effect of asymmetric nonuniformity. This equivalent perturbation problem is solved iteratively in the frequency domain, and the corresponding time-domain behavior is obtained via inverse Fourier transform. Moreover, upon consideration that local perturbations negligibly impact on far-end differential mode (DM) quantities, the uniform DL model with averaged p.u.l. parameters is used for the SI performance evaluation of transmitted DM voltages in SPICE, showing that comparable results can be obtained while avoiding the cumbersome implementation of a nonuniform transmission line topology. The methodology is applied to the prediction of the eye diagram degradation for a 20 Gbps transmission through a microstrip DL subject to geometrical asymmetry and nonuniformity.

Index Terms—Eye diagram, differential lines, mode conversion, nonuniform transmission lines, perturbation approach.

I. INTRODUCTION

Differential signaling is widely used in modern interconnects to mitigate crosstalk and radiated susceptibility/emission, thus improving signal integrity (SI) and electromagnetic compatibility (EMC) performance in high-speed links. Ideally, a best-practice differential line (DL) design consists of a geometrically balanced (i.e., symmetrical) and uniform coupled multiconductor transmission line (MTL) matched to the corresponding differential mode (DM) impedance.

However, nonuniformity is often introduced due to layout constraints [1]. In addition, manufacturing variability can introduce a geometrical asymmetry in the conductor shape as well as further nonuniformity causing, e.g., the shape to vary along the direction of propagation [2]. Asymmetry causes the propagation characteristics along the two line conductors to differ. It was shown that asymmetry indeed plays a detrimental role in worsening the SI of the transmitted DM signals, and

also gives rise to DM-to-common mode (CM) conversion, in a similar fashion as crosstalk [3] and termination imbalance [4] do. Moreover, nonuniformity causes a variation of the DM impedance over the line length.

In this paper, the detrimental effects of nonuniformity and asymmetry on the overall time-domain performance of DLs are analyzed by means of a perturbation approach [5], [6], starting from a reference line with averaged per-unit-length (p.u.l.) parameters. The actual deviation of the p.u.l. parameters from the average configuration is accounted for by means of equivalent distributed sources along the reference line. The resulting problem is solved in the frequency domain, and the corresponding time-domain behavior is obtained by inverse Fourier transform.

Moreover, since it is observed that local perturbations have a negligible impact on far-end DM voltages, the reference uniform line is used as an approximate model to simulate the same configuration in SPICE, showing that comparable accuracy on the eye pattern characteristics is achieved without the need for resorting to a cumbersome nonuniform line implementation.

The technique is applied to the simulation of the eye diagrams for a 20 Gbps transmission over a microstrip DL with increasing deviations from the ideal best-practice (i.e., uniform and symmetric) design.

II. PROPOSED PERTURBATIVE APPROACH

The frequency-domain equations for a coupled nonuniform MTL read [7]

$$\frac{d}{dz}\mathbf{V}(f, z) = -\mathbf{Z}(f, z)\mathbf{I}(f, z) \quad (1a)$$

$$\frac{d}{dz}\mathbf{I}(f, z) = -\mathbf{Y}(f, z)\mathbf{V}(f, z) \quad (1b)$$

where f denotes the frequency, $z \in [0, \ell]$ is the longitudinal coordinate, $\mathbf{V} = [V_1, V_2]^T$ and $\mathbf{I} = [I_1, I_2]^T$ collect the voltages and currents along the two conductors in phasor form, respectively, whereas \mathbf{Z} and \mathbf{Y} are the pertinent place-dependent p.u.l. impedance and admittance matrices, respec-

tively. For compatibility with SPICE simulations, these p.u.l. matrices are expressed as

$$\mathbf{Z}(z, f) = \mathbf{R}_{dc}(z) + \sqrt{f} (1 + j) \mathbf{R}_{hf}(z) + j\omega \mathbf{L}_{dc}(z) \quad (2a)$$

$$\mathbf{Y}(z, f) = \mathbf{G}_{dc}(z) + f \mathbf{G}_{hf}(z) + j\omega \mathbf{C}_{dc}(z) \quad (2b)$$

where $\omega = 2\pi f$ is the angular frequency, $\mathbf{G}_{hf}(z) = 2\pi \tan \delta \mathbf{C}_{dc}(z)$ and an average loss tangent is used for inhomogeneous media.

For a geometrically balanced DL, the *modal* counterpart of (1) describing the propagation of the DM and CM turns out to be decoupled [3]. This implies that if a pure DM source is applied (consisting of two equal sources opposite in phase at the terminations of the physical conductors), only the DM is excited and the propagation is virtually free of mode conversion, while DM degradation is avoided by matching the line to the DM characteristic impedance, hereafter denoted by Z_{DM} .

A. Perturbative Effect of Asymmetry and Nonuniformity

The solution of the nonuniform MTL equation (1) is typically achieved numerically, by approximating the line as a cascade of uniform subsections. In the remainder of this work, this approach is referred to as the uniform cascade subsection (UCS) method. Following the perturbative approach in [5], [6] instead, the place-dependent p.u.l. impedance and admittance matrices in (1) are expressed as a deviation from their average value along the line, i.e.,

$$\mathbf{Z}(f, z) = \bar{\mathbf{Z}}(f) + \Delta \mathbf{Z}(f, z), \quad \bar{\mathbf{Z}}(f) = \frac{1}{\ell} \int_0^\ell \mathbf{Z}(z, f) dz \quad (3a)$$

$$\mathbf{Y}(f, z) = \bar{\mathbf{Y}}(f) + \Delta \mathbf{Y}(f, z), \quad \bar{\mathbf{Y}}(f) = \frac{1}{\ell} \int_0^\ell \mathbf{Y}(z, f) dz \quad (3b)$$

In turn, voltages and currents are also expressed as a sum of perturbation terms, i.e.,

$$\mathbf{V}(f, z) = \mathbf{V}_0(f, z) + \sum_k \mathbf{V}_k(f, z) \quad (4a)$$

$$\mathbf{I}(f, z) = \mathbf{I}_0(f, z) + \sum_k \mathbf{I}_k(f, z) \quad (4b)$$

with $k > 0$.

The starting (reference) solution is found as the solution of

$$\frac{d}{dz} \mathbf{V}_0(f, z) = -\bar{\mathbf{Z}}(f) \mathbf{I}_0(f, z) \quad (5a)$$

$$\frac{d}{dz} \mathbf{I}_0(f, z) = -\bar{\mathbf{Y}}(f) \mathbf{V}_0(f, z) \quad (5b)$$

i.e., a uniform MTL with the averaged p.u.l. parameters, whereas the perturbation terms are the solution of

$$\frac{d}{dz} \mathbf{V}_k(f, z) = -\bar{\mathbf{Z}}(f) \mathbf{I}_k(f, z) - \Delta \mathbf{Z}(f, z) \mathbf{I}_{k-1}(f, z) \quad (6a)$$

$$\frac{d}{dz} \mathbf{I}_k(f, z) = -\bar{\mathbf{Y}}(f) \mathbf{V}_k(f, z) - \Delta \mathbf{Y}(f, z) \mathbf{V}_{k-1}(f, z) \quad (6b)$$

i.e., the same uniform MTL as in (5), but with additional distributed sources. The perturbation terms are computed iteratively, starting from the reference solution of (5) and by suitably updating the distributed sources in the right-hand side

of (6). A closed-form solution, involving integration of the distributed sources, is available for (6) [7]. At each frequency, the iterations are terminated when the relative contribution of the perturbations \mathbf{V}_k and \mathbf{I}_k falls below a given threshold.

B. Time-Domain Response

For the prediction of the SI performance, the time-domain voltage responses are also cast in the form of a perturbation:

$$\mathbf{v}(t) = \mathbf{v}_0(t) + \sum_k \mathbf{v}_k(t) \quad (7)$$

where \mathbf{v}_0 corresponds to the time-domain response of the reference DL (5) with averaged p.u.l. parameters. Owing to the linearity of the Fourier transform operator $\mathcal{F}(\cdot)$, the contributions in (7) are obtained as $\mathbf{v}_k(t) = \mathcal{F}^{-1}\{\mathbf{V}_k(f)X(f)\}$, for $k \geq 0$, where $X(f)$ denotes the spectrum of the time-domain input source, whereas the terms $\mathbf{V}_k(f)$ are computed in the frequency domain, as outlined in Section II-A, for a unitary source. Specifically, for eye diagram simulation, as considered in the following application example, $X(f)$ is the spectrum of the transmitted pseudo-random bit sequence.

III. APPLICATION EXAMPLE

The outlined approach is applied to the SI analysis of the microstrip DL depicted in Fig. 1. The left panel shows the overall line configuration, with a differential signaling applied at the near-end ($z = 0$) termination, and with all conductors terminated by $Z_0 = Z_{DM}/2$ for DM matching. To model digital input stages at the receiver side, additional 0.3-pF capacitors are parallel-connected at the far-end ($z = \ell$) termination. A length of $\ell = 15$ cm is considered. The central panel of Fig. 1 shows the cross-section of the DL. Ideally, the width of the left and right traces should be equal and, together with their separation, uniform along the line length (i.e., constant with z).

However, as illustrated by the top view in the right panel of Fig. 1, the width and separation may in general vary along the line, for instance as a result of manufacturing variability or layout constraints. In the following, three different test cases are generated by increasing perturbation of the geometry with respect to the ideal configuration (referred to as test case 0). Different values for the trace widths and separation are defined at the start and end points of the line, as indicated in Table I, and a linear variation of the conductor shape is assumed between these points. The remaining parameters, taken from [1], are $h = 1.524$ mm, $t = 35$ μ m, $\epsilon_r = 3.66$, $\sigma = 41$ MS/m and $\tan \delta = 0.003$. For each test case, the p.u.l. parameters (2) are evaluated in HSPICE with the internal field solver at 200 intermediate cross-sections.

Fig. 2 shows the DM and CM voltage transfer functions calculated in MATLAB for test case #3 by means of the perturbation technique outlined in Section II-A (dashed red lines). For comparison, the results obtained with the subdivision of the DL in UCSs (solid blue lines) are also provided, showing very good agreement between the two techniques.

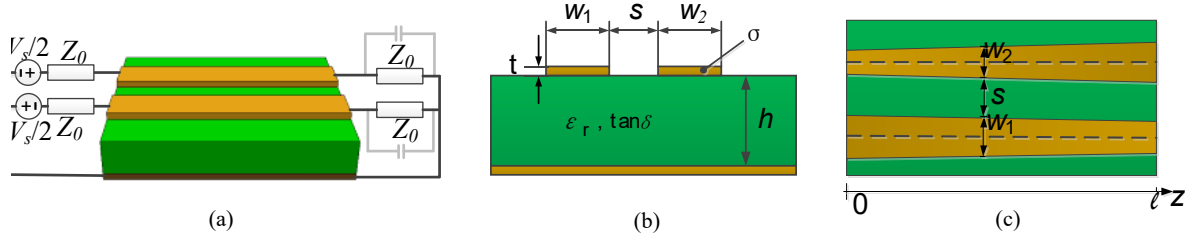


Fig. 1. Layout of the microstrip DL: (a) overall configuration with line terminations; (b) cross-sectional view; (c) top view with asymmetry and nonuniformity.

TABLE I
TRACE WIDTHS AND SEPARATION AT THE START AND END POINTS OF THE MICROSTRIP DL FOR THE CONSIDERED TEST CASES. UNITS ARE IN MM.

	$z = 0$			$z = \ell$		
	w_1	w_2	s	w_1	w_2	s
test case 0	1.8	1.8	0.7	1.8	1.8	0.7
test case 1	2.05	1.1	0.925	2.4	1.45	0.575
test case 2	2.75	0.9	0.675	2.4	1.15	0.725
test case 3	3	0.7	0.65	2.65	0.95	0.7

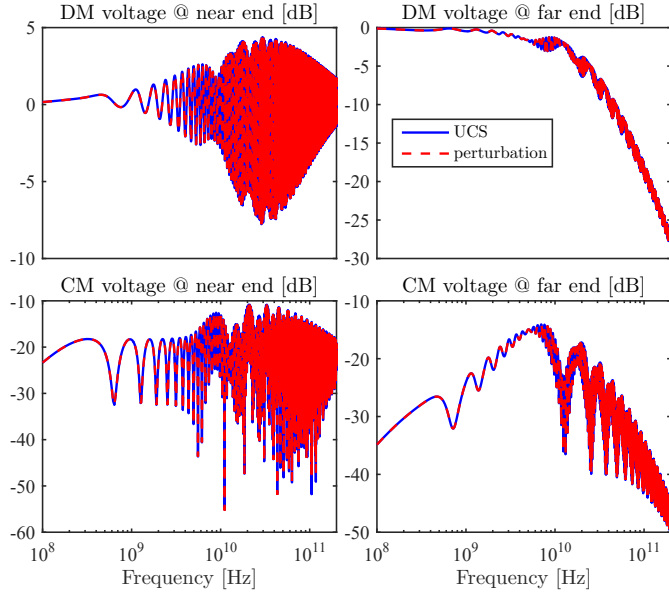


Fig. 2. Frequency-domain behavior of the DM and CM voltages at the DL terminations computed for test case #3 with both the UCS method (solid blue lines) and the perturbation approach (dashed red lines).

A. Eye Diagram Simulation

In terms of modal quantities, casting voltages and currents at line terminals as in (4) allows putting in evidence the fact that if nonuniformity is weak (as in the case of manufacturing variability), only its average effect (i.e., the average contribution accounted for by the matrices in (3)) appreciably impacts on DM voltages at the far end. Conversely, the local variation of the actual p.u.l. parameters around the average values in (3) is generally negligible. As an explicative example, for the three

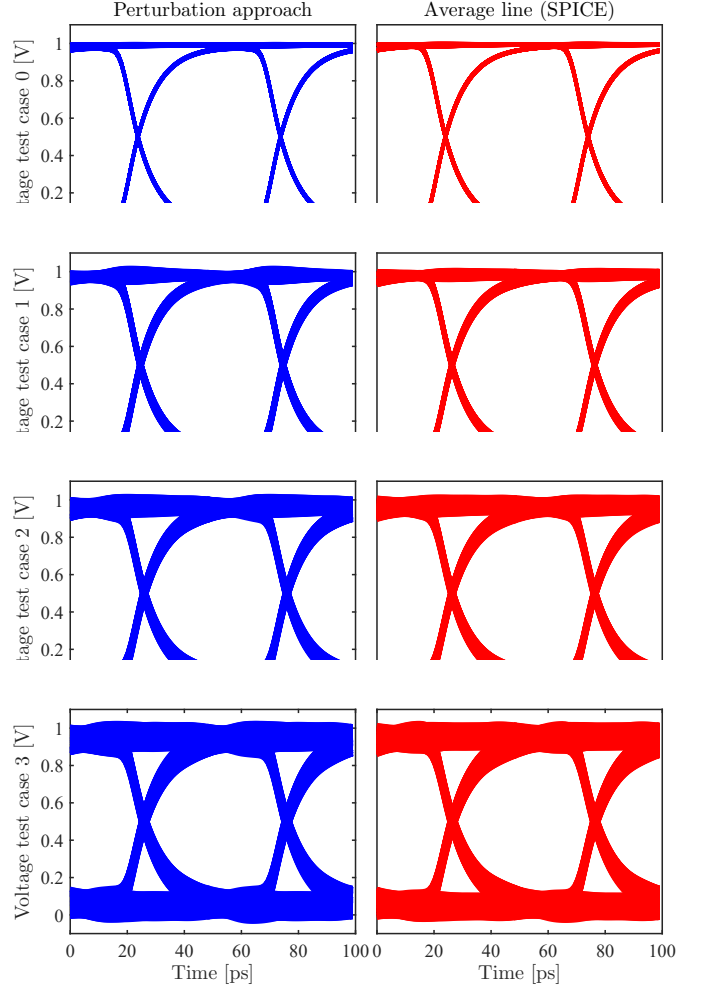


Fig. 3. Eye diagrams for a 20 Gbps bit stream simulated for the different DL configurations in Table I by means of the perturbation approach (left column, blue plots) and the SPICE simulation of the uniform DL with averaged p.u.l. parameters (right column, red plots).

test cases in Table I, the maximum difference over the entire frequency band between the complete perturbative solution and the initial solution of the reference line with averaged p.u.l. parameters (5) is collected in Table II for the near- and far-end DM and CM voltages. Unlike for the other modal quantities, for the far-end DM voltage the observed difference turns out to be rather small. Hence, the simulation of the

uniform line with averaged p.u.l. parameters (5) is expected to provide sufficiently accurate results in the SI investigations of transmitted signals.

TABLE II
MAXIMUM DIFFERENCES BETWEEN THE COMPLETE PERTURBATIVE SOLUTION AND THE SOLUTION OF THE REFERENCE UNIFORM LINE, IN DB.

	near-end DM	far-end DM	near-end CM	far-end CM
test case 1	5.93	0.86	26.4	17.2
test case 2	1.50	0.25	26.9	17.4
test case 3	1.79	0.35	34.6	20.7

To prove this, the frequency-domain responses of the four configurations in Table I are evaluated by the proposed perturbation approach (complete solution), and they are used to estimate the corresponding eye diagrams for the differential transmission of a pseudo-random bit sequence at 20 Gbps with rise/fall times of 5 ps. The results are collected in the left column of Fig. 3 (blue plots). In addition, the eye diagrams obtained from the transient SPICE simulation of the uniform DL with averaged p.u.l. parameters (5) are shown in the right column (red plots). As better illustrated from the metrics in Table III, a reasonable estimation of the eye characteristics is indeed achieved by means of this approximate model, despite the large perturbation of the geometry. This confirms that a uniform model with averaged p.u.l. parameters suffices, in a first instance, to perform the far-end SI assessment of an asymmetric and nonuniform DL without the need for a cumbersome implementation of a nonuniform line topology. It should be noted that the difference for test case 0 is to be merely ascribed to numerical errors, as there is no nonuniformity (and hence, no perturbation) in the DL.

The results in Fig. 3 show that for the ideal configuration of a symmetric and uniform DL (i.e., test case 0), the eye pattern is very open even for high bitrates. As the geometry is increasingly perturbed and deviates from such an ideal layout, however, the eye progressively degrades.

TABLE III
EYE DIAGRAM FEATURES ESTIMATED VIA THE PERTURBATION APPROACH AND THE TRANSIENT SPICE SIMULATION OF THE DL WITH AVERAGED P.U.L. PARAMETERS.

	Eye height [V]			Eye width [ps]		
	perturbation	SPICE	error	perturbation	SPICE	error
test case 0	0.912	0.914	0.2%	49.7	49.6	0.2%
test case 1	0.866	0.859	0.8%	48.6	48.9	0.6%
test case 2	0.794	0.791	0.4%	48.0	48.1	0.2%
test case 3	0.727	0.725	0.3%	47.2	47.3	0.2%

IV. CONCLUSIONS

This paper discusses a novel approach to perform SI assessments for DLs affected by asymmetric and nonuniform geometry. The technique is based on calculating the response as a perturbation of the response of a uniform DL with averaged p.u.l. parameters. The time-domain perturbative contributions are computed by inverse Fourier transform of the corresponding frequency-domain perturbations, thus readily allowing for the inclusion of frequency-dependent losses.

The technique is applied to the SI investigation of a microstrip DL with increasing perturbation of the geometry with respect to the ideal case of uniform and symmetric conductors. The resulting degradation of the eye diagram for the transmission of a 20 Gbps bit sequence is assessed.

Moreover, even for large perturbations of the geometry, the effect of local nonuniformity does not significantly impact on the DM voltage at the far end. Therefore, it is shown that the transient SPICE simulation of the reference uniform line with averaged p.u.l. parameters provides comparable far-end results, and can be therefore regarded as an approximate, yet accurate model that avoids the simulation of a nonuniform line topology.

ACKNOWLEDGMENT

This work was partially supported by the Research Foundation Flanders (FWO-Vlaanderen), of which Dr. Manfredi is a Postdoctoral Research Fellow.

REFERENCES

- [1] C. Gazda, D. Vande Ginste, H. Rogier, R.-B. Wu, and D. De Zutter, "A wideband common-mode suppression filter for bend discontinuities in differential signaling using tightly coupled microstrips," *IEEE Trans. Adv. Packag.*, vol. 33, no. 4, pp. 696–978, Nov. 2010.
- [2] P. Manfredi, D. Vande Ginste, and D. De Zutter, "An effective modeling framework for the analysis of interconnects subject to line-edge roughness," *IEEE Microw. Wireless Compon. Lett.*, vol. 25, no. 8, pp. 502–504, Aug. 2015.
- [3] F. Grassi, Y. Yang, X. Wu, G. Spadacini, and S. A. Pignari, "On mode conversion in geometrically unbalanced differential lines and its analogy with crosstalk," *IEEE Trans. Electromagn. Compat.*, vol. 57, no. 2, pp. 283–291, Apr. 2015.
- [4] F. Grassi, G. Spadacini, and S. A. Pignari, "The concept of weak imbalance and its role in the emissions and immunity of differential lines," *IEEE Trans. Electromagn. Compat.*, vol. 55, no. 6, pp. 1346–1349, Dec. 2013.
- [5] M. Chernobryvko, D. Vande Ginste, and D. De Zutter, "A two-step perturbation technique for nonuniform single and differential lines," *IEEE Trans. Microw. Theory Techn.*, vol. 61, no. 5, pp. 1758–1767, May 2013.
- [6] P. Manfredi, D. De Zutter, and D. Vande Ginste, "Analysis of nonuniform transmission lines with an iterative and adaptive perturbation technique," *IEEE Trans. Electromagn. Compat.*, vol. 58, no. 3, pp. 859–867, Jun. 2016.
- [7] C. R. Paul, *Analysis of Multiconductor Transmission Lines*. New York: Wiley, 1994.